



Title	Nanophase separation and structural evolution of block copolymer films: a "green" and "clean" supercritical fluid approach
Author(s)	Ghoshal, Tandra; Biswa, Subhajit; O'Regan, Colm; Holmes, Justin D.; Morris, Michael A.
Publication date	2014-11-18
Original citation	Ghoshal, T., Biswas, S., O'Regan, C., Holmes, J. D. and Morris, M. A. (2015) 'Nanophase separation and structural evolution of block copolymer films: A "green" and "clean" supercritical fluid approach', Nano Research, 8(4), pp. 1279-1292. doi: 10.1007/s12274-014-0616-7
Type of publication	Article (peer-reviewed)
Link to publisher's version	http://dx.doi.org/10.1007/s12274-014-0616-7 Access to the full text of the published version may require a subscription.
Rights	© Tsinghua University Press and Springer-Verlag Berlin Heidelberg 2014. This is a pre-print of an article published in Nano Research. The final authenticated version is available online at: https://doi.org/10.1007/s12274-014-0616-7
Item downloaded from	http://hdl.handle.net/10468/5336

Downloaded on 2018-08-23T19:32:59Z

Nanophase Separation and Structural Evolution of Block Copolymer Films: A “Green” and “Clean” Supercritical Fluid Approach

Tandra Ghoshal, Subhajit Biswas, Colm O'Regan, Justin D. Holmes* and Michael A. Morris*

¹Materials Chemistry and Analysis Group and Materials Research Group, Department of Chemistry and Tyndall National Institute, University College Cork, Cork, Ireland. ²Centre for Research on Adaptive Nanostructures and Nanodevices (CRANN/AMBER), Trinity College Dublin, Dublin, Ireland

[*] Corresponding Author: Prof. Justin D. Holmes

Tel: +353(0)21 4903608

Fax: +353(0)21 4274097

E-mail: j.holmes@ucc.ie

Prof. Michael A. Morris

Tel: + 353 21 490 2180

Fax: +353 21 427 4097

E-mail: m.morris@ucc.ie

ABSTRACT: Thin films of block copolymers (BCPs) are widely accepted as potentially important materials in a host of technological applications including nanolithography. In order to induce domain separation and form well-defined structural arrangements, many of these are solvent-annealed (i.e. solvent swollen) at moderate temperatures. The use of solvents can be challenging in industry from an environmental point of view as well as having practical/cost issues. However, a simple and environmentally friendly alternative to solvo-thermal annealing is described herein. Various asymmetric polystyrene-*b*-poly(ethylene oxide) (PS-*b*-PEO) thin films were annealed in a compressible fluid, supercritical carbon dioxide (scCO₂), to control nano-domain orientation and surface morphologies. For the first time, periodic well defined, hexagonally ordered films were demonstrated using a supercritical fluid process at low temperatures and pressures. Predominant swelling of PEO domain in scCO₂ induces nanophase separation. scCO₂ serves as green alternative to the conventional organic solvents for the phase segregation of BCPs with complete elimination of any residual solvent in the patterned film. The depressurization rate of scCO₂ following annealing was found to affect the morphology of the films. The supercritical annealing conditions could be used to define nanoporous analogues of the microphase separated films without additional processing providing a one-step route to membrane like structures without affecting the ordered surface phase segregated structure. An understanding of the BCP self-assembly mechanism can be realized in terms of the deviation in glass transition temperature, melting point, viscosity, interaction parameter and volume fraction of the constituent blocks in the scCO₂ environment.

INTRODUCTION

The self assembly of nanoscale materials to hierarchically ordered structures offers new opportunities in the development of miniaturized optical, electronic, optoelectronic and magnetic devices.¹ Block copolymers can self-assemble into periodic domains via a process of microphase separation²⁻³ and these systems, with controlled orientation and ordering have promise in a number of applications including nanolithography, membrane synthesis and nanofluidics.⁴⁻⁷ Solvent annealing of BCP films is an effective approach for obtaining ordered phase-separated thin films at low temperatures and in relatively short time periods since the solvent swells the polymer, creating free volume and providing the necessary chain mobility to the polymer blocks.⁸⁻⁹ Generally, organic and halogenated solvents are preferred to swell one or more blocks within a polymer film,¹⁰ even though they are toxic and have a negative environmental impact. Removal of excess solvent is necessary for many technological and biological applications because of performance sensitivity.¹¹⁻¹⁵ Also, the effect of solvent annealing on the structure and orientation of BCP films can often be unpredictable.⁹ Furthermore, achieving a stable ordered structure with a controlled orientation throughout a very large area of a substrate is challenging. In contrary, supercritical carbon dioxide (scCO₂) provides an attractive solvent alternative because of its low cost, wide availability, moderate critical conditions (critical temperature (T_c)= 31°C, critical pressure (P_c)=73.8 bar and critical density (ρ_c) = 0.468g/cm³), environmentally and chemically (volatile, inert, non-flammable) benign nature.¹⁶ Particularly attractive properties of scCO₂ for BCP solvo-annealing include: gaslike diffusivities and tunability of the solvent strength (providing diverse selectivity to polymers) through pressure and temperature control, low interfacial tension and complete elimination of the gas after process termination.¹⁷

scCO₂ is known as an important polymer processing aid which causes substantial reduction in polymer viscosity resulting from the dissolution of the gas in a polymer¹⁸ thereby decreasing the glass transition temperature (T_g 's) dramatically¹⁹ The effects of scCO₂ on the phase

behaviour of bulk and thin film BCPs might be expected to be complicated since selective block swelling can change the volume fraction, f , the Flory-Huggins interaction parameter, χ due to the differences in polymer-CO₂ interaction which effectively modify the kinetics of phase segregation and substantially affect wetting behaviour.²⁰⁻²³ In addition, for self-assembly of BCP thin films, the compressibility of scCO₂ could be tuned through the manipulation of pressure and temperature allowing selectivity towards a specific block, significantly improving the ordering of well defined nanostructures.²⁴ scCO₂ can also be used to fabricate nanocellular structures and nanopores in block copolymer thin and thick films.^{5, 25-28}

Much attention has been paid to ordering and kinetics of BCP thick and thin films by scCO₂, examined from both a theoretical and an experimental perspective.^{23, 25, 29-30} However, to-date surface periodic arrangements of two blocks has only been realized by annealing polymers above their melting points.^{25, 30-31} Here, we demonstrate the formation of periodic BCP arrangements via solvo-annealing in compressible scCO₂ at low temperatures avoiding crystallization effects. The structural and morphological evolution of BCP thin films, upon selective swelling of one of the blocks, was examined as a function of temperature, pressure and annealing time. Furthermore, ordered nanopores could also be introduced into the polymeric thin films through the scCO₂ annealing process without the use of external reagents such as methanol.²⁵

EXPERIMENTAL

Polystyrene-*b*-poly(ethylene oxide) (PS-*b*-PEO) diblock copolymers were purchased from Polymer Source and used without further purification (number-average molecular weight, M_n , PS = 42 kg mol⁻¹, PEO = 11.5 kg mol⁻¹, M_w/M_n = 1.07 and PS = 16 kg mol⁻¹, PEO = 5 kg mol⁻¹, M_w/M_n = 1.04 M_w : weight-average molecular weight). Single crystal B doped p-type silicon (100) wafers with a native oxide layer were used as a substrate. These wafers were cleaned by

ultrasonication in acetone and toluene for 30 minutes in each solvent and dried under a nitrogen stream. PS-*b*-PEO was dissolved in toluene to yield a 1 wt% polymer solution which was aged for 12 h at room temperature. A PS-*b*-PEO thin film was formed by spin coating the polymer solution (3000 rpm for 30 s) onto a Si wafer. The polymer coated wafer was subsequently loaded into a stainless steel high pressure vessel (5 ml.), which was sealed and placed into a preheated oven at a certain temperature range varying from 35° C to 60°C and pressurized with CO₂ at a rate 0.5ml min⁻¹, using a manual pressure generator (ISCO HPLC pump). Annealing of the polymer thin films was carried out in scCO₂ at a constant temperature of the oven and pressure (80-140 bar). After the desired time, the annealing chamber was removed and cooled naturally before the CO₂ pressure was released at a rate 2 bar min⁻¹ with a pressure controller. Experiments were conducted at various temperatures, pressures and depressurization rates.

Surface morphologies of BCP thin films were imaged by scanning probe microscopy (SPM, Park systems, XE-100) in tapping mode and scanning electron microscopy (SEM, FEG Quanta 650). The film thicknesses were measured by optical ellipsometer (Woolam M2000) and electron microscopy. Samples were prepared for TEM cross-sectional imaging with an FEI Helios Nanolab 600i system containing a high resolution Elstar™ Schottky field-emission SEM and a Sidewinder FIB column and were further imaged by transmission electron microscopy (TEM, JEOL 2100).

RESULTS AND DISCUSSION

EFFECT OF SCF PRESSURE ON MICROPHASE SEPARATION:

A block copolymers used in this study was polystyrene-*b*-poly(ethylene oxide) (PS-*b*-PEO) (16-5) with PEO as the minority cylinder forming block in a PS matrix. No ordering of BCP thin films was observed for the non-annealed, spin coated samples or after annealing under either vacuum or in CO₂ at less than 80 bar (temperature range 35-50° C). The absence of any nanoscopic ordering of the films indicates that the polymer has insufficient mobility for

microphase separation under these conditions (see supporting information Figure S1). Note that no evidence for dewetting droplets associated with structural instability of the films, following extended annealing (2 h) in vacuum, was observed probably due to the strong preferential chemical interaction of PEO with the polar Si/SiO_x substrate.³² The effect of scCO₂ on the phase segregation of the PS-PEO (16-5) BCP at 80-140 bar and 45° C is shown in the AFM images given in Figure 1. At the lowest pressure of 80 bar (Figure 1a), the film starts to phase segregate and discontinuous line-like patterns with random arrays of PEO cylinders become visible. Consistent with previous studies,^{14, 32} the PEO block appears darker in the AFM image due to its much lower glass transition temperature (T_g) (-60° C) compared to 105° C for PS. At scCO₂ pressures of 100 and 120 bar, microphase separated periodic ordered arrangements of PEO domains, lying parallel to the substrate plane in a PS matrix were formed (Figures 1b and 1c) over large areas of the substrate. No large scale surface roughness or thickness undulation across the surface was noticed. At a scCO₂ pressure of 140 bar (Figure 1d) enhanced surface roughness, thickness variations (indicated by bright regions) and pattern degradation (pattern missing) were observed. The ellipsometry measured thickness of the films before and after annealing was constant at 35 nm. PS as well as PEO blocks can be swollen by CO₂, but the film shrinks back to its original thickness after complete removal of CO₂. The PEO domain repeat period calculated from the fast-Fourier transform (FFT) of the AFM images was 22 nm and this value (+/- 2%) was observed for all films studied. The repeat period of 22 nm is significantly less than the reported value for this particular block copolymer solvent annealed in organic solvents, *i.e.* 25 nm,³³⁻³⁴ implying either the absence of any trapped residual solvent *i.e.* complete removal of the annealing solvent (CO₂). Thus, a CO₂ pressure range between 100-120 bar was optimum for the microphase separation of (PS(16)-PEO(5k)).

EFFECT OF ANNEALING TEMPERATURE ON MICROPHASE SEPARATION:

The effects of annealing temperature on the microphase separation and ordering of BCP was examined as small change in temperature alters the behaviour (dissolution of CO₂ into the polymer) of the polymer-fluid mixture under the same pressure.³⁵ Figure 2 shows AFM images of PS-PEO thin film clearly indicating that the microphase separation occurs at all temperature investigated *i.e.* between 35-50 °C and at a constant pressure of 100 bar. However, at lower temperatures, (35 °C and 40 °C), although the film did not dewet, the fingerprint patterns formed showed short domain lengths (of the order of few nanometers) and were of poor quality (discontinuous patterns) as shown in Figures 2a and b. Increasing the temperature to 45 and 50 °C yielded longer domain persistence lengths (~ μm) of the PEO domains as shown in Figures 2c and d. The repeat period and film thickness essentially remained unchanged for all the samples annealed at the different temperatures. The striped patterns were formed up to a certain temperature limit of 60 °C at 100 bar, but no long range ordered patterns were observed at this temperature and the films became highly roughened.

MICROPHASE SEPARATION OF HIGHER MOLECULAR WEIGHT BCP:

To examine the general applicability of the scCO₂ annealing approach, a higher molecular weight PS-*b*-PEO (42-11.5) polymer system was investigated. A lower scCO₂ pressure of 80 bar and a lower temperature of 40°C could be used to induce microphase separation compared to the lower molecular weight (16-5) polymer (see supporting information, Figure S3), although the patterns formed were quite disordered, with both vertical and parallel orientation of the PEO cylinders being observed. Achievement of microphase separated structures at relatively lower temperatures and pressures, compared to the low molecular weight polymer, is probably simply due to the higher value of χN (41.49) (χ is the Flory-Huggins interaction parameter and N is the degree of polymerization) for the (42-11.5) system, hence involves lower external mediating or thermodynamic driving force is required to achieve phase

separation compared to χ_N (16.28) for the lower molecular weight polymer. The solubility of a block copolymer generally falls between that of its two homopolymers.²⁹ As various authors have reported that the solubility of scCO₂ of polymers is only significantly influenced by pressure and temperature and almost independent of the molar mass of PS and PEO,^{31, 35-36} it seems unlikely that the cause of enhanced phase separation is related to a swelling effect leading to greater free volume and increased chain mobility.

ROLE OF SCF ON MICROPHASE SEPARATION:

The microphase segregation and ordering of the PS-PEO block copolymer systems in scCO₂ could be achieved over a lower temperature (45-50° C) and pressure (100-120 bar) range as depicted in Figures 1 and 2. One important aspect in explaining the microphase segregation of PS-PEO upon scCO₂ annealing is the glass transition temperature (T_g) and pressure (T_p) of the BCP, generally observed as intermediate values of the corresponding blocks. In this context, T_g and T_p for PS is significant compared to PEO as PEO is a semi-crystalline polymer and its transition values resides far below from the experimental temperatures and pressures employed in this study. Detailed studies on CO₂ induced devitrification pressure and temperature for a PS thin film revealed a larger depression of both T_g and T_p for a certain amount of scCO₂.³⁷ This would be consistent with the fact that there is an effective increase of the interaction of scCO₂ with the polymer thin film for a given temperature and pressure compared to vacuum annealing. The scCO₂ interaction with the BCP thin film is controlled by the overall CO₂ solubility in the entire film, which includes CO₂ at the free surface and substrate regions (interfaces) and in the interior of the film. Previous reports suggests that the polar PEO layer will preferentially wet the substrate surface (favourable PEO-substrate interactions) whilst PS will segregate to the air interface to form a PS-rich layer (PS has a lower surface energy, $\gamma_{PS} = 33 \text{ mNm}^{-1}$; $\gamma_{PEO} = 43 \text{ mNm}^{-1}$).³² The sorption of scCO₂ in PEO is found to be in between 20-

25 wt%, which is larger than that of PS (5-6 wt%) at a pressure of 100 bar.^{36, 38-39} Thus, enhanced swelling of the PEO domain is expected compared to the PS block. CO₂ also interacts favourably with the hydroxyl groups on the SiO_x/Si substrate, with the effect of screening the segmental interactions of the polymer with the substrate. However, the enhancement of CO₂ sorption in the interior of the film (preferentially within the PEO blocks) compared to the substrate-polymer and polymer-air interfaces possibly overcomes the screening of undesirable surface interactions or film dewetting. The increased mobility of the PEO block chains has the effect of increasing the configurational freedom (lower packing segmental density) of chain segments which leads to an increase in the free energy within the film. This higher solvent concentration inside the film is balanced by the segregation of the PEO blocks to the air interface in order to reduce the surface tension. Thus, both the PS and PEO blocks were present at the polymer-air interface upon exposure to scCO₂. Moreover, the value of χ_N is larger for a thin film than for a bulk polymer and this value further increases in the presence of scCO₂.³⁷ Regardless of the film thickness, increased disparity between the CO₂-PS and CO₂-PEO interactions corresponds to a larger effective interaction parameter (χ_{eff}), leading to phase separation. The solubility of CO₂ in both the PS and PEO homopolymers has previously been reported to decrease with increasing temperature and increases with increasing pressure,^{36, 38} which is consistent with the fact that the interactions between polymers and CO₂ become less favourable with increasing temperature, lowering the probability of phase separation. These previous studies also explain why lower temperatures (< 50° C) are more suitable to achieve phase separation at a constant pressure. Our experimental observations support the previous findings that the solubility of CO₂ in PEO is highest at a temperature of 43°C and at a pressure of 100 bar.³⁸ Microphase separation would be favoured at higher pressures but this causes a larger depression in the melting temperature of the polymers. Specifically, the melting temperature decreases monotonically with increasing the CO₂ pressure,⁴⁰ thereby increasing

the mobility of the PEO blocks which can cause deformation in the surface structure. In our experiment, the structural deformation was observed at 140 bar and no microphase separation was realized above this pressure. The process of the forming ordered patterns by scCO₂ annealing is relatively faster than the literature values for solvent (organic) annealing times.³⁴ This is due to the vigorous reduction of viscosity of PEO chains during annealing which helps the scCO₂ to diffuse within the block and reach a critical value, permitting the polymer chains can easily extend and/or relax to achieve phase separation. When the samples were depressurized to ambient condition, CO₂ diffused from the interface between the films and substrate maintaining the ordered surface structure.

EFFECT OF ANNEALING TIME ON MICROPHASE SEPARATION:

The scCO₂ solvo-anneal period is also an important parameter for the long term stability of the ordered patterns at room temperature. When the anneal period is increased to 1 h (Figure 3a), continuous striped patterns with PEO cylinders lying parallel to the substrate surface were observed. Compared to longer annealing time of (1 h), films annealed for shorter annealing time (30 min) exhibits lower defect densities and smoother surface at similar temperature and pressure (see Supporting information – Figure S2). Exposure of the polymer films to scCO₂ for 1 h 30 m, flipped the PEO cylinders to vertical orientation and hexagonal ordered dot patterns were formed (Figure 3b). The repeat cylinder- to- cylinder distance was 20 nm which is smaller compared to the striped pattern repeat distance of 22 nm. The dot patterns remained stable for an annealing period up to 2 h (Figure 3c). The film thickness also essentially remained unchanged during morphological transition. This transformation in the cylinder orientation of PEO suggests that the structures achieved are not the thermodynamically stable state (morphology) of the film. With sufficient solvent uptake, the films swell and reach a critical thickness where a parallel arrangement is more thermodynamically favourable. However, the

film cannot expand infinitely with the additional solvent exposure, so the cylinders flip to vertical direction in order to maintain a constant solvent concentration, through a deswelling process where the excess solvent is released. The effective decrease of the repeat cylinder distance for the vertical orientation also supports this hypothesis. The release of solvent might be associated with the minimization of the surface energy differences of the film, or because of internal strain differences between the vertical and parallel arrangements. The similarity in thicknesses for two different final film structures also indicates the complete removal of CO₂ at the end of the process; otherwise slightly thicker swelled films would be obtained.

MORPHOLOGY AND INTERFACES:

Cross-sectional TEM imaging provided a means to further examine the morphology and interfaces of the scCO₂ annealed BCP films deposited on the Si substrates. The similarity of the PS (1.05 g cm⁻³) and amorphous PEO (1.12 g cm⁻³) densities resulted in featureless TEM micrographs for the microphase separated films after annealing for 30 min in scCO₂ at a pressure of 100 bar (See supporting information – Figure S4), suggesting that scCO₂ solvo-annealing does not result in PEO crystallization, even though the annealing temperatures are higher than the melting point (29.3 °C) in a scCO₂ environment. Since the crystalline form of PEO has a significantly higher density (1.24 g cm⁻³)⁴¹ than amorphous PEO (1.12 g cm⁻³) it would be expected to provide more contrast for TEM imaging.⁴² In order to observe contrast between the ordered nanofeatures, a plasma dry etch process was applied to partially remove the PEO domains which were further prepared for cross-sectional TEM analysis. The SEM image (Figure 4a) demonstrates ordered striped patterns with a 22 nm domain spacing, similar to unetched samples measured by AFM (in Figure 1b). However, etch treatment, deformation or discontinuity in the line patterns was observed due to a non-selective dry etch process, suggesting physical damage to the patterns had occurred. Pattern damage is supported by TEM

data (Figure 4b) where the film thickness was 25 nm, reduced from its original value of 35 nm due to etching. The arrangement of the PEO domain across the film thickness, which continues to a definite depth within the film could not be defined due to the partial etching of the domains. The average spacing of features was consistent with a domain spacing of 22 nm as previously measured by SEM. The wave structure was not perfectly periodic due to either/or both the non-selective nature of the etch and/or a non-perfect image projection (since the film may not have been cut exactly orthogonal to the stripes). A higher magnification image (bottom image of Figure 4b) revealed the average diameter of the PEO domain was 12 nm, which were broadened during the etching step. The film was well adhered to the substrate surface with no indication of deformation or delamination.

EFFECT OF DEPRESSURIZATION RATE:

As previously mentioned, T_g 's of block copolymers in scCO₂ decreases dramatically, which plays an important role in their microphase separation to create an ordered arrangement. Additionally, quenching of the samples to room temperature before depressurization of the scCO₂ from the cell in order to preserve the ordered structure is required. As T_g of PEO is always below the room temperature and T_g of PS is reported to be around 30°C in scCO₂ environment,⁴³ the films typically lack the physical robustness to survive depressurization. Li et al.³¹ reported that the higher depressurization rates affect the structural ordering, by increasing the number of depressions or holes on the surface of a film, ultimately resulting in the pattern deformation. The effects of a faster depressurization rate ($> 2 \text{ bar min}^{-1}$) on the external and internal structural transition of the BCP films were investigated at a CO₂ pressure of 100 bar and a temperature of 45°C for 30 minutes, released at a rate of 5 bar min^{-1} . The AFM image in Figure 5a shows the expected ordered structure with the addition of several dark spots or holes throughout the film surface (see supporting information, Figure S5). These holes arise

from the rapid depressurization of the fluid as the gas forces its way to the film surface. The SEM image shown in Figure 5b represents the ordered surface patterns with holes. For SEM imaging, the sample was achieved by treating the film with ethanol to etch and/or modify the PEO domains in order to increase the electron contrast.^{32, 34} A cross-sectional TEM image obtained from the same sample highlights the surface and internal morphology of the film (inset of Figure 5b). At the surface of the film, undulating patterns similar to those seen in Figure 4b were observed. Within and throughout the interior of the film, a well-resolved array of equally spaced ordered pores could be observed (inset of Figure 5b) consistent with the expected removal of the PEO domain by the ethanol treatment^{14, 32}. The pore width was measured to be around 8 nm. Multiple layers of voids or spaces can be seen across the film thickness (Figure 5c). The voids are either continuous parallel layers to the film surface or elliptical ordered patterns, depending on the orientation of the PEO cylinders. The measured film thickness was 50 nm, consistent with ellipsometry data. The PEO blocks were predominantly swelled by scCO₂, which escaped during fast depressurization, introducing void spaces inside the films and providing additional volume or thickness to the film. Another reason for the void generation could be sudden increase in the viscosity of the polymers during fast depressurization. The diameters of the nanopores has a strong correlation with the diameters of the cylindrical PEO domains, due to selective swelling of PEO domains by scCO₂. Larger pore widths were observed compared to the diameter of the PEO domains because of the increased swelling of the PEO domains at high scCO₂ depressurization rates (5 bar min⁻¹ compared to 2 bar min⁻¹). The average diameter of the nanopores was 11 nm. Furthermore, increasing the scCO₂ pressure (> 120 bar) together with the faster release rate (> 5 bar min⁻¹) resulted in the collapse of the ordered surface structure of the BCP film. Hence, in our experiment, a scCO₂ pressure of 120 bar was the optimum pressure with a depressurization rate of 5 bar min⁻¹ for introducing nanopores within the BCP thin film with an ordered surface arrangement.

DISCUSSION:

The mechanism for generating the ordered nanopores within the BCP thin film could be rationalized by considering the solubility of scCO₂ within the films. The solubility of scCO₂ within these polymer (PS-PEO, PS and polyethylene glycol (PEG) homopolymers of molecular weight of 17 kg mol⁻¹ and 4 kg mol⁻¹ respectively) thin films was examined by annealing them in scCO₂ solvo-atmosphere for 30 minutes at different temperatures and pressures, subject to a pressure release rate 5 bar min⁻¹. Spectroscopic ellipsometry was used to measure the thicknesses of the films before and after scCO₂ exposure to estimate swelling, assuming uniaxial expansion of the film based on equation 1:

$$Sw\% = \frac{\Delta V}{V_0}(\%) = \frac{h-h_0}{h_0} \times 100\% \quad (1)$$

Here, V_0 is the initial volume of the film, h is the thickness of the swollen film, and h_0 is the initial thickness of the polymer film. Data are summarized in Figure 6 and Table 1 (see Supporting Information). For the polymer films investigated, their thickness increased with increasing pressure and with decreasing temperature. Hence the solubility of CO₂ in the films also decreased with increasing temperature and increased with increasing pressure. The role of the scCO₂ is to interfere with the polymer attractive forces that tend to swell the chains: acting as a ‘screen’. The screening affect largely depends on the solvent density, *i.e.* the higher the solvent density, the better is the screening. When the pressure is increased at a constant temperature, the density of CO₂ and therefore the screening are also increased. However, increasing temperature leads to a decrease in screening as the dilation of SCF is much faster than that of polymer (the thermal expansion coefficient of the SCF is higher). The data also suggest that the scCO₂ predominantly swells the PEO compared to the PS, as slight variations were observed for the PS homopolymer (Figures 6a-d). During fast depressurization, the PEO expanded extensively to around 150% of its original volume, causing significant strain around

the domain interface since the expansion of the PS block is below 10 %, eventually leading to pore formation. The sum of swelling measured individually for the PS and PEO component was plotted against temperature and pressure which shows a very little deviation from the measured (by ellipsometry) swelling values for PS-PEO thin film. Note that the measured statistics is correct only for the particular experimental settings used (temperature 35-50 ° C and pressure 80-140 bar). Further increasing the CO₂ pressure may not be advantageous for introducing nanopores within the film because these pores begin to connect to each other as porosity increases. Attachment or aggregation of these nanopores causes deformation of the film and surface structures. The mechanism for generating the nanopores within the BCP thin film by scCO₂ solvo-annealing may not be limited only for the BCP thin film but could be potentially applicable to other monolithic specimens.

The role of scCO₂ (as for any other solvent) is to penetrate the polymer and screen the attractive forces between the chains, increasing free volume and sponsoring chain mobility and hence microphase separation.⁹ The phase separation of a diblock copolymer (A-b-B) is typically determined by the interaction parameter, χ_{AB} , the molecular weight, N and fractional volume composition of polymer blocks, f . However, for a BCP thin film in a scCO₂ environment, the effective interaction parameter will change as shown in equation 2:⁴⁴⁻⁴⁵

$$\chi_{eff}N \sim \phi(\chi_{PS-PEO} + \Delta\chi)N = \phi(\chi_{PS-PEO} + (\chi_{PS-S} - \chi_{PEO-S}))N \quad (2)$$

Here, ϕ is the volume concentration of the copolymer in the solvent (S) and $\Delta\chi$ is the difference between PS-solvent and PEO-solvent interaction parameters. As discussed earlier, scCO₂ is a selective solvent for PEO and thus, its effects on the compatibility of PS-PEO systems can be complicated due to interplay between ϕ and $\Delta\chi$. Hence, the fractional volume composition of the PS block and the effective interaction parameter will also be changed by swelling according to the equation 3:⁴⁴⁻⁴⁵

$$f_{PS} \sim f_{PS}\varphi \quad (3)$$

On the basis of eq. (3), selective swelling of PEO by CO₂ decreases the effective volume fraction of the PS blocks, *i.e.* f_{PS} decreases. However, since, f_{PS} lies in the cylindrical phase region in vacuum, further decreasing the effective volume fraction will not change the equilibrium phase structure. According to equation (2), CO₂ annealing introduces two competing terms to $\chi_{eff}N$. Firstly, the overall copolymer volume fraction in the presence of scCO₂, φ , which is less than 1 and second, a positive $\Delta\chi$, due to preferential interaction between PEO and CO₂. Generally, large differences between the two polymer-solvent interaction parameters ($\Delta\chi$ is large and positive) increases the $\chi_{eff}N$ value which causes the BCP to change from a disordered state into an ordered state. In other words, if the $\Delta\chi$ effect dominates, the contribution resulting from φ is less than unity and phase separation can be induced by adding selective annealing solvents. In our case, the observed CO₂ induced phase separation relative to vacuum annealing (no phase separation) at the same temperature suggests that the $\Delta\chi$ effect is dominant, therefore, $(\chi_{eff}N)_{CO_2} > (\chi N)_{VAC}$. Thus, effective increase in the interaction parameter under scCO₂ compared to vacuum, leads to phase separation of the BCP thin film.

The trend of swelling of the BCP thin film with temperature and pressure followed the expected variations seen for other systems, but is worth comparing the changes in swelling or volume fractions for the PS to PEO ratio with temperature and pressure.^{23, 29, 31} Figure 7 shows the ratio of swelling for PS:PEO as a function of pressure and temperature, highlighting that the ratio decreases with pressure (Figure 7a) and increases with temperature (Figure 7b). These data are attributed to the fact that the rate of increase or decrease of swelling of PEO with pressure and temperature respectively is much faster than that of PS. scCO₂ is generally described as hydrophobic, however, as the solvent parameter of scCO₂ increases with pressure becoming more hydrophilic and hence favouring the dissolution of more polar PEO compared to PS.⁴⁶ The observed relative increase in the swelling rate of PEO is due to increased

diffusivity with pressure. The diffusion coefficient of PEO increases with scCO₂ pressure⁴⁷ which increases the mobility of the polymer chains, thereby increasing the solubility of scCO₂ into the polymer causing extra free volume to the polymer or swelling. A reverse dependence is seen for the relative swelling of PS to PEO with temperature (Figure 7b) as the PEO domains are predominantly affected by the temperature.

CONCLUSION

In summary, microphase separated PS-b-PEO thin films with surface periodically ordered nanostructures were realized by annealing in a compressible supercritical carbon dioxide (scCO₂) environment at low temperature. scCO₂ clearly demonstrate a green alternative to hazardous organic solvents. Significantly, a morphological transition was observed where PEO cylinders flipped from a parallel to a perpendicular orientation, without disrupting the long range order, with longer scCO₂ exposure times. Higher temperatures and pressures resulted in pattern degradation and surface roughening of the films, whereas low temperatures and pressures were beneficial for forming well-ordered nanostructured arrangement. This scCO₂ annealing method was also applicable to different molecular weight systems. scCO₂ predominantly interacts with the PEO blocks imparting higher mobility and surface energy, responsible for the microphase separation. The effective increase in the interaction parameter and decrease of the glass transition temperatures of the BCP films under scCO₂, compared to vacuum, also leads to phase separation of the BCP thin film. Nanopores or nanocellular structures could be introduced into the films with a periodic surface arrangement by solely using scCO₂ without the use of any other solvent. The complete elimination of the scCO₂ at the end of the process makes the films useful for many technological and biological applications. This unique approach to achieve well ordered nanostructured surface arrangements could be applied in other BCP systems to explore the fundamentals and improve the quality of nanoelectronic devices.

AUTHOR INFORMATION

Corresponding Authors

*Email: j.holmes@ucc.ie; m.morris@ucc.ie

Notes

The authors declare no competing financial interest.

ACKNOWLEDGEMENTS

We acknowledge financial support from the Science Foundation Ireland (Grants: Semiconductor Research Corporation 2011-IN-2194, 09/IN.1/I2602, 12/RC/2278, 09/SIRG/I1621 and CSET CRANN). The contribution of the Foundation's Principal Investigator support is also acknowledged. The authors also thankful to Prof. C. Sinturel for his valuable suggestions.

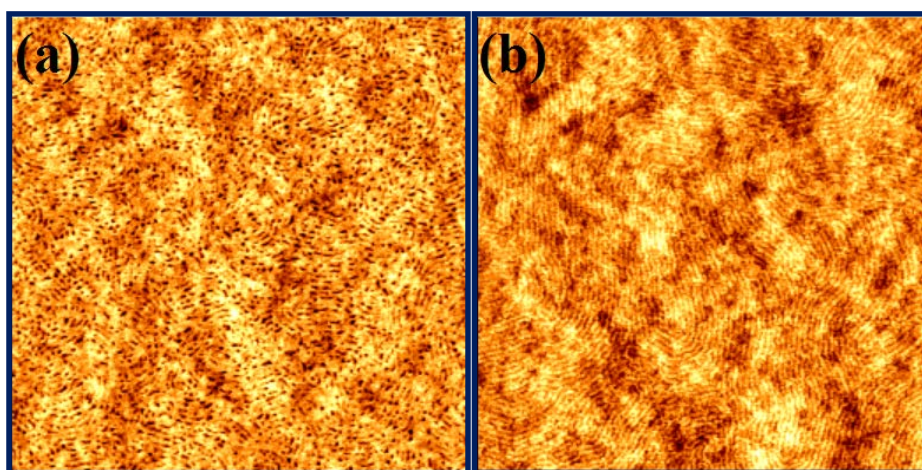
REFERENCES

- (1) Whitesides, G. M.; Mathias, J. P.; Seto, C. T. *Science* **1991**, *254*, 1312-1319.
- (2) Park, C.; Yoon, J.; Thomas, E. L. *Polymer* **2003**, *44*, 6725-6760.
- (3) Bates, F. S.; Fredrickson, G. H. *Phys. Today* **1999**, *52*, 32-38.
- (4) Yao, L.; Woll, A. R.; Watkins, J. J. *Macromolecules* **2013**, *46*, 6132-6144.
- (5) Pai, R. A.; Humayun, R.; Schulberg, M. T.; Sengupta, A.; Sun, J. N.; Watkins, J. J. *Science* **2004**, *303*, 507-510.
- (6) Gu, Y. B.; Dorin, R. M.; Wiesner, U. *Nano Lett.* **2013**, *13*, 5323-5328.
- (7) Serghei, A.; Zhao, W.; Wei, X.; Chen, D.; Russell, T. P. *Eur. Phys. J.-Spec. Top.* **2010**, *189*, 95-101.

- (8) Zhao, J. C.; Jiang, S. C.; Ji, X. L.; An, L. J.; Jiang, B. Z. *Polymer* **2005**, *46*, 6513-6521.
- (9) Mokarian-Tabari, P.; Collins, T. W.; Holmes, J. D.; Morris, M. A. *ACS Nano* **2011**, *5*, 4617-4623.
- (10) Huang, W. H.; Chen, P. Y.; Tung, S. H. *Macromolecules* **2012**, *45*, 1562-1569.
- (11) Padinger, F.; Brabec, C. J.; Fromherz, T.; Hummelen, J. C.; Sariciftci, N. S. *Opto-Electron. Rev.* **2000**, *8*, 280-283.
- (12) Koegler, W. S.; Patrick, C.; Cima, M. J.; Griffith, L. G. *J. Biomed. Mater. Res.* **2002**, *63*, 567-576.
- (13) Ghoshal, T.; Fleming, P. G.; Holmes, J. D.; Morris, M. A. *J. Mater. Chem.* **2012**, *22*, 22949-22957.
- (14) Ghoshal, T.; Maity, T.; Godsell, J. F.; Roy, S.; Morris, M. A. *Adv. Mater.* **2012**, *24*, 2390-2397.
- (15) Ghoshal, T.; Senthamaraikannan, R.; Shaw, M. T.; Holmes, J. D.; Morris, M. A. *Nanoscale* **2012**, *4*, 7743-7750.
- (16) DeSimone, J. M. *Science* **2002**, *297*, 799-803.
- (17) Reverchon, E.; Adami, R. *J. Supercrit. Fluids* **2006**, *37*, 1-22.
- (18) Tomasko, D. L.; Li, H. B.; Liu, D. H.; Han, X. M.; Wingert, M. J.; Lee, L. J.; Koelling, K. W. *Ind. Eng. Chem. Res.* **2003**, *42*, 6431-6456.
- (19) Wissinger, R. G.; Paulaitis, M. E. *J. Polym. Sci. Pt. B-Polym. Phys.* **1991**, *29*, 631-633.
- (20) Vogt, B. D.; RamachandraRao, V. S.; Gupta, R. R.; Lavery, K. A.; Francis, T. J.; Russell, T. P.; Watkins, J. J. *Macromolecules* **2003**, *36*, 4029-4036.
- (21) Watkins, J. J.; Brown, G. D.; RamachandraRao, V. S.; Pollard, M. A.; Russell, T. P. *Macromolecules* **1999**, *32*, 7737-7740.
- (22) RamachandraRao, V. S.; Gupta, R. R.; Russell, T. P.; Watkins, J. J. *Macromolecules* **2001**, *34*, 7923-7925.

- (23) Arceo, A.; Green, P. F. *J. Phys. Chem. B* **2005**, *109*, 6958-6962.
- (24) Shah, M.; Pryamitsyn, V.; Ganesan, V. *J. Phys. Chem. B* **2007**, *111*, 402-407.
- (25) Zhang, R.; Yokoyama, H. *Macromolecules* **2009**, *42*, 3559-3564.
- (26) Gong, J. L.; Zhang, A. J.; Bai, H.; Zhang, Q. K.; Du, C.; Li, L.; Hong, Y. Z.; Li, J. *Nanoscale* **2013**, *5*, 1195-1204.
- (27) Hanrahan, J. P.; Copley, M. P.; Ziegler, K. J.; Spalding, T. R.; Morris, M. A.; Steytler, D. C.; Heenan, R. K.; Schweins, R.; Holmes, J. D. *Langmuir* **2005**, *21*, 4163-4167.
- (28) Hanrahan, J. P.; Copley, M. P.; Ryan, K. M.; Spalding, T. R.; Morris, M. A.; Holmes, J. D. *Chem. Mat.* **2004**, *16*, 424-427.
- (29) Chen, Y.; Koberstein, J. T. *Langmuir* **2008**, *24*, 10488-10493.
- (30) O'Driscoll, B. M. D.; Griffiths, G. H.; Matsen, M. W.; Hamley, I. W. *Macromolecules* **2011**, *44*, 8527-8536.
- (31) Li, Y.; Wang, X. C.; Sanchez, I. C.; Johnston, K. P.; Green, P. F. *J. Phys. Chem. B* **2007**, *111*, 16-25.
- (32) Ghoshal, T.; Shaw, M. T.; Bolger, C. T.; Holmes, J. D.; Morris, M. A. *J. Mater. Chem.* **2012**, *22*, 12083-12089.
- (33) Xu, J.; Hong, S. W.; Gu, W. Y.; Lee, K. Y.; Kuo, D. S.; Xiao, S. G.; Russell, T. P. *Adv. Mater.* **2011**, *23*, 5755-5761.
- (34) Ghoshal, T. M., T; Senthamaraikannan, R; Shaw, M; Carolan, P; Holmes, J; Roy, S; Morris, M. *Scientific Reports* **2013**, *3*, 2772.
- (35) Gourgouillon, D.; da Ponte, M. N. *Phys. Chem. Chem. Phys.* **1999**, *1*, 5369-5375.
- (36) Zhang, Y.; Gangwani, K. K.; Lemert, R. M. *J. Supercrit. Fluids* **1997**, *11*, 115-134.
- (37) Pham, J. Q.; Johnston, K. P.; Green, P. F. *J. Phys. Chem. B* **2004**, *108*, 3457-3461.
- (38) Weidner, E.; Wiesmet, V.; Knez, Z.; Skerget, M. *J. Supercrit. Fluids* **1997**, *10*, 139-147.
- (39) Guadagno, T.; Kazarian, S. G. *J. Phys. Chem. B* **2004**, *108*, 13995-13999.

- (40) Madsen, L. A. *Macromolecules* **2006**, *39*, 1483-1487.
- (41) Chen, W. Y.; Zheng, J. X.; Cheng, S. Z. D.; Li, C. Y.; Huang, P.; Zhu, L.; Xiong, H. M.; Ge, Q.; Guo, Y.; Quirk, R. P.; Lotz, B.; Deng, L. F.; Wu, C.; Thomas, E. L. *Phys. Rev. Lett.* **2004**, *93*, 028301-028304.
- (42) Michler, G. H., *Electron Microscopy of Polymers* Springer: **2008**, 978-3-540-36350-7.
- (43) Wang, W. C. V.; Kramer, E. J.; Sachse, W. H. *J. Polym. Sci. Pt. B-Polym. Phys.* **1982**, *20*, 1371-1384.
- (44) Helfand, E.; Tagami, Y. *J. Chem. Phys.* **1972**, *56*, 3592-3598.
- (45) Hanley, K. J.; Lodge, T. P. *J. Polym. Sci. Pt. B-Polym. Phys.* **1998**, *36*, 3101-3113.
- (46) Labuschagne, P. W.; Kazarian, S. G.; Sadiku, R. E. *J. Supercrit. Fluids* **2011**, *57*, 190-197.
- (47) Hrnčić, M. K.; Marković, E.; Trupej, N.; Skerjet, M.; Knez, Z. *J. Supercrit. Fluids* **2014**, *87*, 50-58.



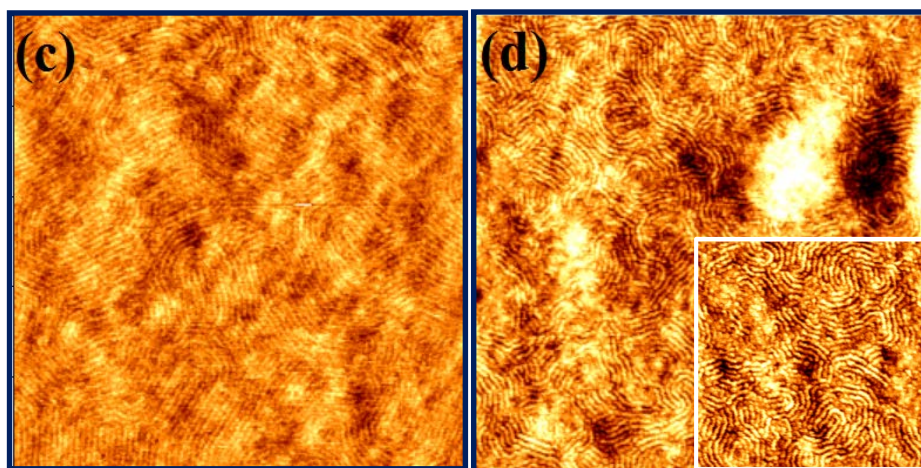


Figure 1 Tapping mode AFM images of PS-PEO (16-5) thin film annealed in a scCO₂ environment at a temperature of 45 °C for 30 m with different scCO₂ pressure of (a) 80 (b) 100 (c) 120 and (d) 140 bar. Scale bar: 2 x 2 μm.

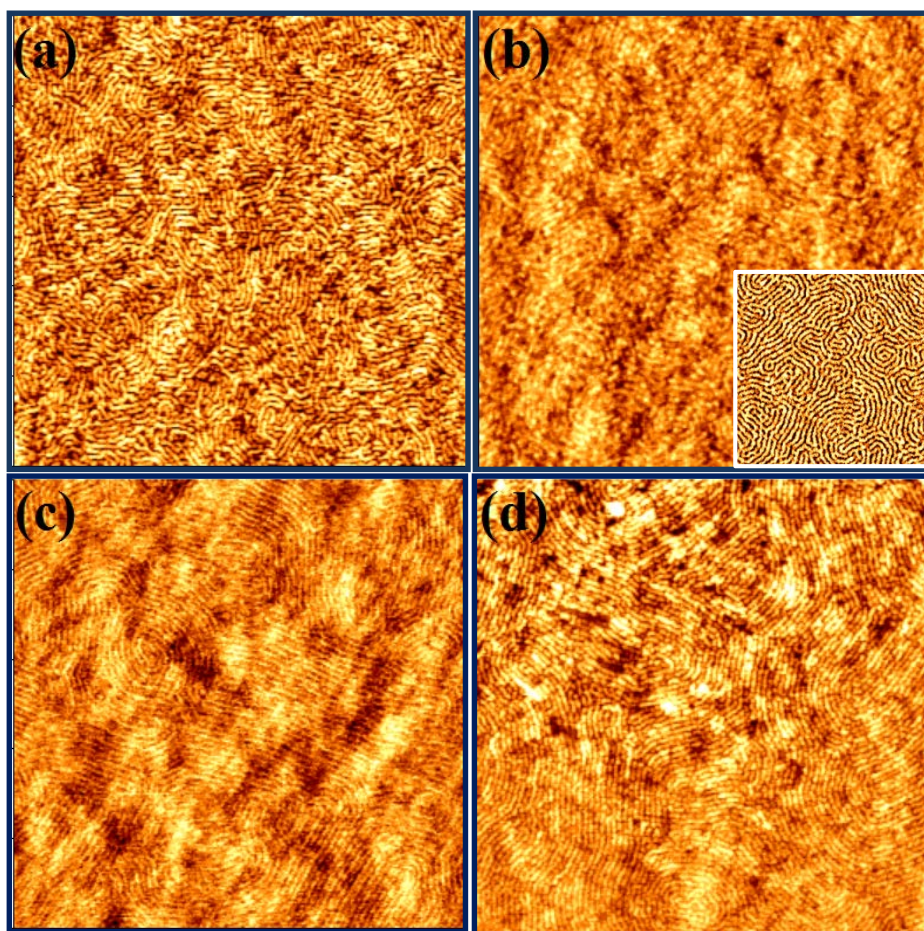


Figure 2 Tapping mode AFM images of PS-PEO (16-5) thin film annealed in a scCO₂ environment at a pressure of 100 bar for 30 m at different temperatures of (a) 35 °C (b) 40 °C (c) 45 °C and (d) 50 °C. Scale bar: 2 x 2 μ m.

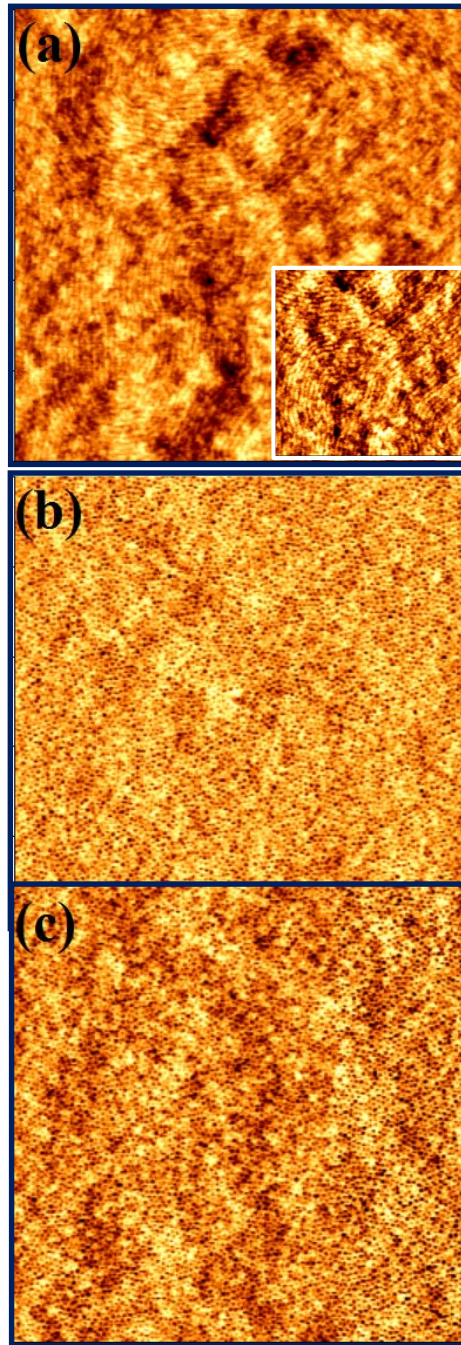


Figure 3 Tapping mode AFM images of a PS-PEO (16-5) thin film annealed in scCO₂ environment at a pressure of 100 bar and at a temperature of 45 °C for (a) 1 h (b) 1 h 30 m and (c) 2 h. Scale bar: 2 x 2 μm.

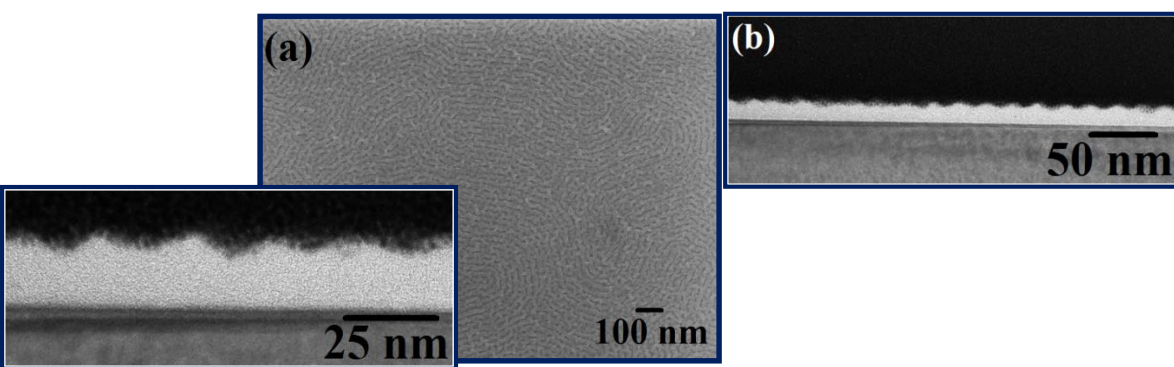


Figure 4 A microphase separated PS-PEO (16-5) thin film annealed in a scCO₂ environment at a pressure of 100 bar and at a temperature of 45 °C for 30 min and partially removed PEO domains by plasma dry etch (a) SEM image and (b) cross-sectional FIB thinned TEM images.

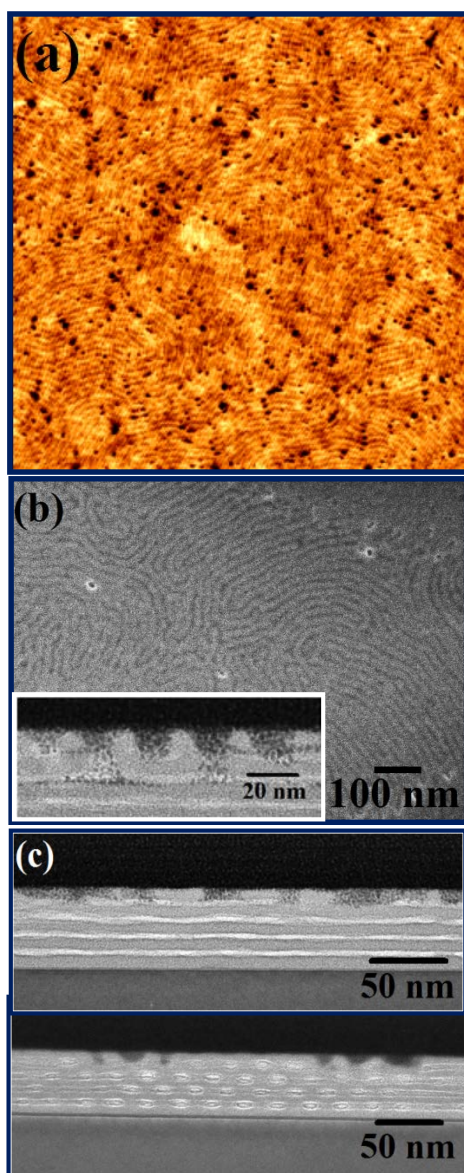


Figure 5 A microphase separated PS-PEO (16-5) thin film annealed in a scCO₂ environment at a pressure of 100 bar and at a temperature of 45 °C for 30 min with a depressurization rate of 5 bar min⁻¹ and partially removed PEO domains by chemical etch: (a) AFM image (b) SEM image and (c) cross-sectional FIB thinned TEM images. Inset of (b) shows PEO cylinder arrangement. (a) Scale bar: 2 x 2 μm.

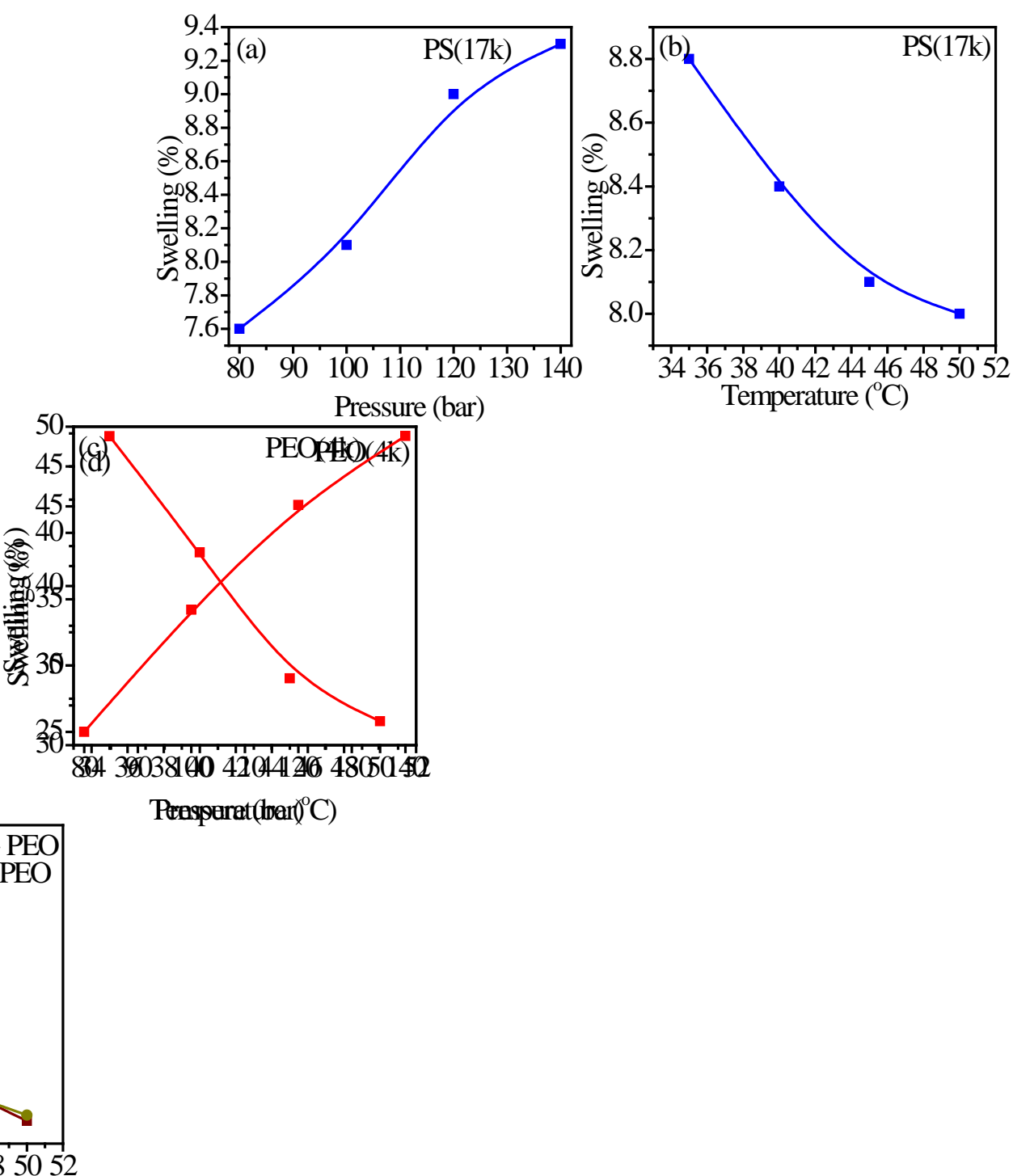


Figure 6 Graphs showing swelling measurements by spectroscopic ellipsometer with annealing temperature and pressure for (a) and (b) PS homopolymer, (c) and (d) PEO homopolymer, (e) and (f) combination of PS and PEO homopolymers and PS-PEO thin films.

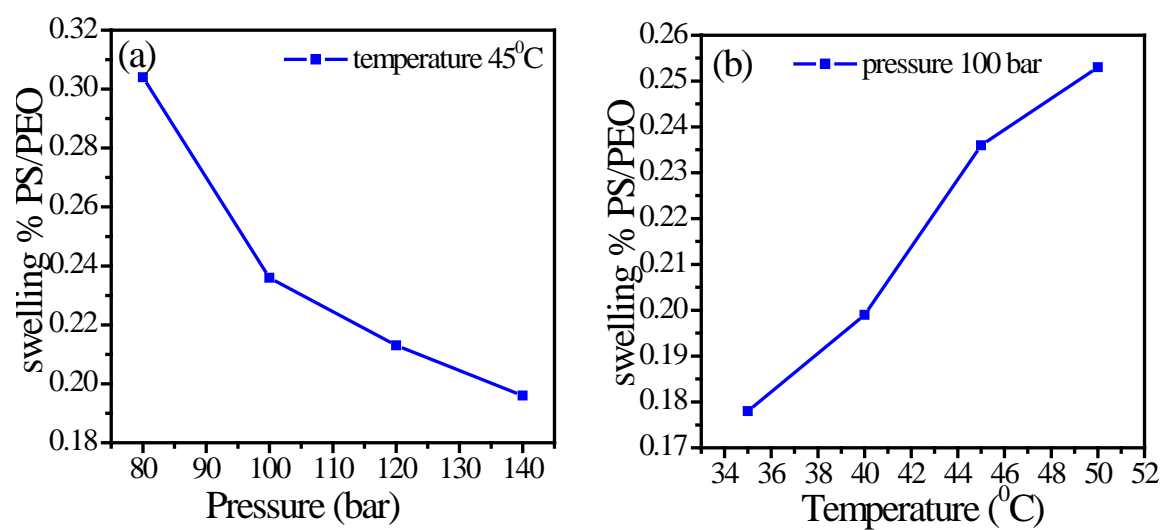
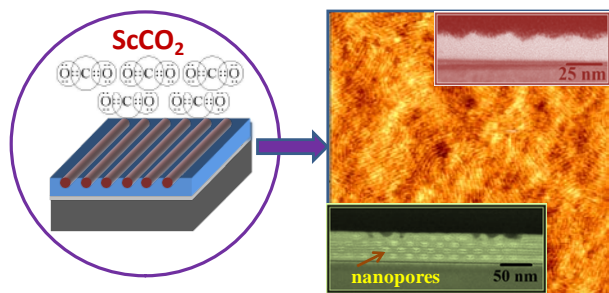


Figure 7 Graphs showing the ratio of swelling for PS:PEO as a function of (a) pressure and (b) temperature.

Table of Contents:



Supercritical carbon dioxide (scCO₂) is described as a green alternative to conventional organic solvents for inducing phase separation and ordering in block copolymer thin films at low temperatures and pressures. Nanopores or nanocellular structures could be introduced into the films. The absence of scCO₂ makes the films useful for many technological and biological applications.